AAC
Journals.ASM.org

Existence of Separate Domains in Lysin PlyG for Recognizing *Bacillus anthracis* Spores and Vegetative Cells

Hang Yang, Dian-Bing Wang, Qiuhua Dong, Zhiping Zhang, Zongqiang Cui, Jiaoyu Deng, Junping Yu, Xian-en Zhang, and Hongping Wei

State Key Laboratory of Virology, Wuhan Institute of Virology, Chinese Academy of Sciences, Wuhan, China

As a potential antimicrobial, the bacteriophage lysin PlyG has been reported to specifically recognize *Bacillus anthracis* vegetative cells only and to kill *B. anthracis* vegetative cells and its germinating spores. However, how PlyG interacts with *B. anthracis* spores remains unclear. Herein, a 60-amino-acid domain in PlyG (residues 106 to 165), located mainly in the previously identified catalytic domain, was found able to specifically recognize *B. anthracis* spores but not vegetative cells. The exosporium of the spores was found to be the most probable binding target of this domain. This is the first time that a lysin for spore-forming bacteria has been found to have separate domains to recognize spores and vegetative cells, which might help in understanding the coevolution of phages with spore-forming bacteria. Besides providing new biomarkers for developing better assays for identifying *B. anthracis* spores, the newly found domain may be helpful in developing PlyG as a preventive antibiotic to reduce the threat of anthrax in suspected exposures to *B. anthracis* spores.

The Gram-positive *Bacillus anthracis* bacterium, causing the disease anthrax in humans, is a well-known bioterrorism agent requiring worldwide medical attention (5, 15, 17, 20, 44). This spore-forming bacterium is a member of the *Bacillus cereus* group, along with *B. cereus*, *Bacillus thuringiensis*, and *Bacillus mycoides* (13). The entire spore of *B. anthracis* is encased by a heavily glycosylated exosporium (10, 43), which functions as a semipermeable barrier and a matrix for binding of molecules involved in defense, germination control, and other interactions of the spores with the environment (18). Under the exosporium is a much thinner coat layer (11, 12, 31, 38), which is critical for resistance properties as well as pathogenic effects (26). Because they are physicochemically stable and resistant to antiseptics, extreme temperature, high pressure, and UV irradiation (3, 33), *B. anthracis* spores are the foremost agent in anthrax threats. Therefore, the control of the spores is of great importance for combating bioterrorism and for the effective treatment of anthrax.

Lysins, produced by bacteriophages to digest the bacterial cell wall for the release of progeny virions, have been considered effective anti-infective agents for control of Gram-positive bacteria (4, 8, 27, 29, 32). PlyG, produced by gamma phage, has been reported to be an effective and specific agent for killing *B. anthracis* vegetative cells (40). The C terminus of PlyG (the site from residue 156 to residue 233) was identified as the cell wall binding domain (CBD), which recognizes vegetative cells, and the N terminus of PlyG (the site from residue 1 to residue 155) was previously considered to be the catalytic domain for destroying the target cells (9). Further research verified that the CBD of PlyG can recognize only the germinating form, but not spores, of *B. anthracis* (9). *In vitro* truncation analysis indicated that the residues from 190 to 199 of PlyG were necessary and sufficient for vegetative cell binding (21, 39). The critical region for the catalytic activity of PlyG (the site from residue 1 to residue 90) was also characterized (22). PlyG has also been reported to kill the germinating form of *B. anthracis* spores (40). However, the mechanism behind this remains unclear, and limited evidence is available on how PlyG interacts with *B. anthracis* spores.

In this study, as a step to understanding how PlyG interacts with *B. anthracis* spores, *in vitro* variant truncated fragments of PlyG were constructed and binding assays were performed to identify whether there is a binding domain in PlyG to recognize *B. anthracis* spores. Surprisingly, a 60-amino-acid fragment located mainly in the previously identified catalytic domain was found to specifically recognize *B. anthracis* spores but not vegetative cells, indicating that PlyG uses different binding domains to recognize spores and cells. These results provide new insight into the mechanism of interaction between PlyG and *B. anthracis* spores and therefore may provide further clues to finding or developing new lysins for controlling *B. anthracis* spores.

MATERIALS AND METHODS

Bacteria. All experiments involving live *B. anthracis* spores and vegetative cells were performed in a biosafety level 3 laboratory. The experimenters were equipped with masks, gloves, and exposure suits. *Bacillus anthracis* A16 was cultured in standard LB medium and harvested as vegetative cells, as reported previously (2, 7, 50). The washed vegetative cells were heat treated for 5 min under boiling water before staining with the truncated proteins and the synthetic peptides. Spores were prepared on modified Difco sporulation medium (DSM), following the procedures described elsewhere (14, 36, 42, 49). The spores were inactivated immediately after harvest with 1% formaldehyde for more than 24 h to make sure of their dormancy during the experiments.

Escherichia coli BL21(DE3) was used for cloning and expression of the recombinant fusion proteins of PlyG and enhanced green fluorescent protein (EGFP). A total of 20 kinds of bacterial strains from 10 genera, comprising 17 bacillus strains and three other Gram-negative bacterial strains,

Received 28 April 2012 Returned for modification 15 May 2012
Accepted 5 July 2012
Published ahead of print 16 July 2012
Address correspondence to Xian-en Zhang, x.zhang@wh.iov.cn, or Hongping Wei, hpwei@wh.iov.cn.
Supplemental material for this article may be found at http://aac.asm.org/.
Copyright © 2012, American Society for Microbiology. All Rights Reserved.
doi:10.1128/AAC.00891-12

were used in the binding selectivity assays, and a subset of these was used as labeling controls for the fluorescence analysis.

Construction of recombinant proteins. The original PlyG gene sequence (GenBank accession no. AF536823) was chemically synthesized by Songon Biotech (Shanghai, China). Fragments from PlyG were genetically fused with the N terminus of EGFP, and eight corresponding expression plasmids, pET-EP9, pET-EP0, pET-EP3, pET-EC3, pET-EC5, pET-EC6, pET-EC8, and pET-EG1, were constructed (see Table S1 in the supplemental material). To obtain active PlyG, the plasmid pBAD-plyG was created (see Table S1). All the resulting clones were confirmed by sequencing.

Synthetic peptides. Three synthetic peptides (see Table S1) were used in the binding assay, with an N-terminal fluorescein isothiocyanate (FITC) modification. One peptide with an N-terminal cysteine was used to react with 20 nm Au nanoparticles (BBI).

Protein expression and purification. The recombinant proteins were expressed in the *E. coli* BL21(DE3) strain in standard LB medium and purified following procedures described previously (40, 54), with minor modifications. For pBAD-containing strains, protein was induced with 0.2% L-arabinose at 16°C for 8 h. Cells were washed, resuspended in 20 mM phosphate buffer at pH 6.6, and lysed with sonication. PlyG, which passed through a HiTrap Q Sepharose FF column (GE Healthcare), bound to a HiTrap SP Sepharose FF column (GE Healthcare) and was eluted in a linear gradient containing 1 M NaCl. For pET-containing strains, protein expression was induced with 1 mM isopropyl β-D-thiogalactoside (IPTG) when an optical density of 0.6 to 0.8 was reached. After induction, the bacteria were incubated overnight at 16°C to allow expression. Purification was achieved through the His_6 tag, following the general protocol using a nickel nitrilotriacetic acid column, washing and eluting with imidazole solutions with concentrations of 60 and 265 mM, respectively. Collected fractions were dialyzed against 1× phosphate-buffered saline (PBS) (137 mM NaCl, 2.7 mM KCl, 4.3 mM $Na_2HPO_4 \cdot H_2O$, 1.4 mM KH_2PO_4, pH 7.4) and then stored at −80°C until use after being quantitated by the Bradford assay using bovine serum albumin (BSA) as a standard.

Staining and microscopy of bacterial cells and spores. To study the binding capabilities of the recombinant proteins, all the bacterial cells and spores tested were stained with the EGFP-tagged truncated proteins and EGFP (as a control), respectively. For bacterial cells, harvested cells were washed twice with 1× PBS by centrifuging (12,000 × *g* for 1 min) and then inactivated by a heat treatment (5 min under boiling water). Then, the cells were reacted with an excess of the EGFP-tagged proteins at 37°C for 30 min to ensure completed labeling. After washing three times with PBSB (1× PBS and 0.1% BSA) by centrifuging (12,000 × *g* for 1 min), the labeled cells were analyzed by using a fluorescence microscope (Delta Vision Personal DV; Applied Precision) and/or a laser scanning confocal microscope (TCS-SP2; Leica, Germany).

For the spores, all were preblocked with PBSM (1× PBS, pH 7.4, and 5% defatted milk powder) at 37°C for 2 h and then washed three times with PBST buffer (1× PBS and 0.05% Tween 20) by centrifuging (12,000 × *g* for 1 min) before staining with PBSB, EGFP, and EGFP-tagged proteins with or without L-alanine and D-alanine, respectively. All *B. anthracis* spores were completely inactivated by 1% formaldehyde after harvest to ensure biosafety and their dormancy state during the staining process, unless otherwise indicated. After reacting with an excess of EGFP and the EGFP-tagged proteins at 37°C for 30 min, the spores were washed three times with PBST buffer by centrifuging (12,000 × *g* for 1 min) before analysis by using the Delta fluorescence microscope. For fluorescence quantitative analysis, the total fluorescence intensity of a special defined region containing only one spore was calculated by the instrument's software automatically. The area of each defined region was fixed in all of the assays, and all the images were captured under the same instrument conditions. The specificity of EP0 was statistically evaluated by comparing the average fluorescence intensity of each spore (>300 spores) with the background fluorescence staining with the buffer PBSB and the control fluorescence staining with EGFP.

SPF assay. A subtraction assay was developed to evaluate the binding affinities of the EGFP-fused truncated proteins for *B. anthracis* cells and spores individually. To achieve this, pretreated *B. anthracis* cells and spores were diluted 10-fold serially and stained with the recombinant truncated proteins for different times at 37°C. Then, the mixtures were centrifuged at 12,000 × *g* for 1 min, and the supernatants (100 μl) were analyzed using a spectrophotofluorometer (SPF) (LS55; Perkin-Elmer) with an excitation wavelength of 488 nm and an emission wavelength of 510 nm. EGFP-fused truncated proteins mixed with PBSB buffer were used as blank controls.

Kinetic analysis of truncated proteins with *B. anthracis* spores. Approximately 5×10^5 biotinylated *B. anthracis* spores were reacted with the streptavidin sensors (ForteBio) at room temperature overnight to ensure complete conjugation prior to analysis. Four truncated proteins, EP0, EP3, EC5, and EC6, and EGFP were tested simultaneously with the spore-modified sensors using an Octet apparatus and its software (ForteBio). It is notable that an on-line blockage strategy with PBSM (1× PBS and 5% defatted milk powder) was used for each sensor (blocked for 10 min, followed by washing with PBS for 3 × 10 min) to reduce nonspecific interactions. Each assay was repeated three times.

Scatchard plot assay. *B. anthracis* spores with a constant concentration of 3.5×10^5 were stained by EC6 with a series of concentrations, ranging from 0.11 to 1.82 μM, at 37°C for 120 min. After centrifugation at 12,000 × *g* for 1 min, the fluorescence of the supernatant of each mixture was read by the SPF assay immediately, using spore-free EC6 solutions as controls. The initial total molar concentration of EC6 was defined as Ct, and the molar concentration of EC6 in the supernatant was defined as Cf, which represents the free proteins that do not bind with the spores. Thus, the molar concentration of the bound protein (Cb) was calculated as (Ct − Cf). For calculation, we assumed that a single spore could be considered a macromolecule, which had a constant mass and volume during the interaction. Therefore, the molar concentration of the spores was defined as Cs, and the binding ratio (ν) was calculated as Cb/Cs. The saturation binding curve was created by fitting the results obtained under a series of dilutions of EC6. Meanwhile, the data were displayed as a Scatchard plot in which the *x* axis was the binding ratio (ν) and the *y* axis was the binding ratio (ν) divided by the free ligand concentration (Cf). According to the principle of this method (34, 52), it is possible to estimate B_{max} and K_d from the Scatchard plot (B_{max} is the *x* intercept, and K_d is the negative reciprocal of the slope). B_{max} represents the maximum ligand number located on a spore for EC6, while K_d represents the binding constant of EC6 interaction with *B. anthracis* spores.

Labeling peptides with AuNPs. Peptide N21 was immobilized on Au nanoparticles (AuNPs) using a procedure described previously (16), with some modifications. Briefly, AuNPs (20 nm, with the pH adjusted to 9.2 before use) reacted with N21 (in H_2O) under vigorous stirring for 12 h to form Au-S bonds that link N21 to Au. After washing three times with a washing buffer (10 mM phosphate buffer, 150 mM NaCl, pH 7.4) to remove unreacted peptides, the N21-AuNP conjugate was stored at 4°C until use.

Transmission electron microscopy. PBSM-blocked *B. anthracis* spores, with or without sonication pretreatment, were reacted with the gold-labeled peptide, N21-AuNPs. The sonication treatment was used to detach part of the exosporium from the spores, and ultracentrifugation was used to purify the sonicated spores from the detached exosporium as described previously (49, 37). After washing three times to remove unbound N21-AuNPs, the sample was analyzed by using a transmission electron microscope (Tecnai G^2 20 Twin; Fei).

***In vitro* lysin activity.** Lysin activity was measured as previously described (32), with some modifications. Briefly, *B. anthracis* strain A16 was grown to an optical density at 600 nm (OD_{600}) of 0.2 to 0.3, centrifuged, and resuspended in phosphate buffer to a final OD_{600} of 0.8 to 1.0. Twofold serial dilutions of purified PlyG (100 μl) were added to a 100-μl bacterial suspension in 96-well plates (Perkin-Elmer), and the drop in the OD_{600} was monitored by using a Synergy H1 spectrophotometer

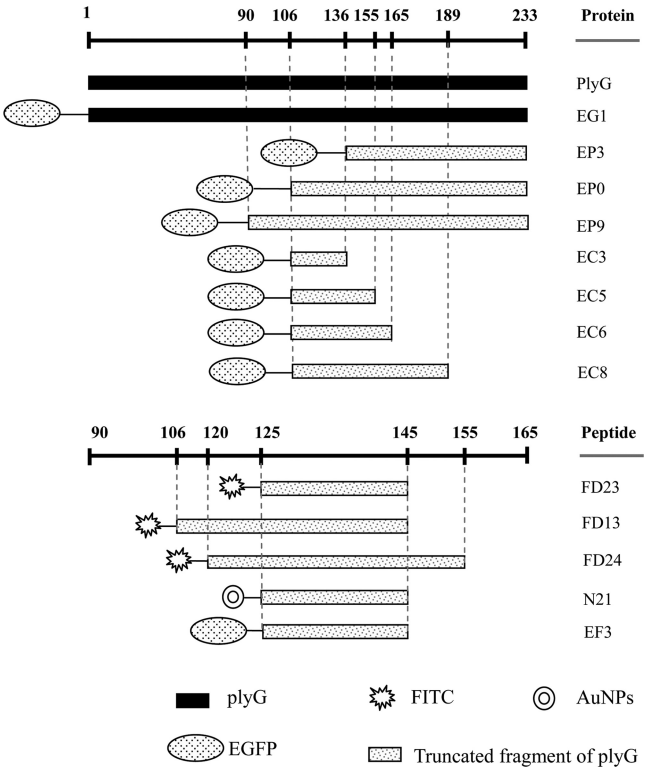

FIG 1 Schematic positions of the truncated proteins and synthetic peptides used in the study.

(BioTek) for 30 min at 37°C. A unit of PlyG activity was defined as the highest dilution that decreased the absorbance by 50% within 15 min (32).

Spore killing assay. The PlyG-mediated spore killing assay was tested in the presence of L-alanine and D-alanine as described previously (40). In brief, aliquots of spores were heat activated at 65°C for 5 min and suspended in 1 ml tryptic soy broth with either 100 mM L-alanine or D-alanine for 5 min at 37°C. Samples were then treated with 10 U PlyG for up to 2 h and finally plated for counting after washing three times with PBS.

RESULTS

Construction and expression of recombinant proteins. The whole PlyG protein contains 233 amino acids. Using standard genetic engineering methods, a series of recombinant proteins and their fusion proteins with EGFP were constructed and expressed as shown in Fig. 1. It was found that these proteins could be well expressed in *E. coli*. After purification and dialysis, the proteins were used directly for the binding assays. Meanwhile, four small peptide fragments were synthesized and labeled with or without FITC to confirm their binding activity.

Recognition of *B. anthracis* cells. To test if the recombinant truncated fusion proteins retained the ability to recognize *B. anthracis* cells, equal numbers of *B. anthracis* cells were stained with the three recombinant proteins EP9, EP0, and EP3 at 37°C for 30 min. The concentrations of the recombinant proteins were chosen within its linear range with the fluorescence intensity. After centrifugation, the supernatants were analyzed using the spectrophotofluorometric (SPF) assay. As shown in Fig. 2A, all three proteins could bind to *B. anthracis* cells, but EP0 displayed a higher binding affinity than the other two.

To optimize the staining time required for complete labeling of *B. anthracis* cells, *B. anthracis* vegetative cells were incubated with EP0 for 0, 10, 20, 30, 60, and 120 min in parallel. Figure 2B shows that 30 min was enough to ensure complete labeling of *B. anthracis* cells with EP0 under the experimental conditions. For a further confirmation of the staining time of *B. anthracis* cells, the corresponding cells of each sample, thoroughly washed three times with PBST buffer (1× PBS and 0.05% Tween 20), were imaged by a fluorescence microscope (see Fig. S1 in the supplemental material). The results showed that after more than 30 min of staining, the fluorescence intensity of each cell reached a maximum. This result was consistent with that of the SPF assays, suggesting that 30 min of staining was enough for complete staining of *B. anthracis* cells by EP0.

Confocal microscopy was also used to determine the binding location of EP0 on *B. anthracis* cells (see Fig. S2 in the supplemental material). The image clearly showed that EP0 can bind directly to the cell wall of *B. anthracis* cells, mediated by CBD of PlyG, rather than permeating the cell.

The lysin PlyG can specifically kill *B. anthracis* cells and has no effect on other *Bacillus* strains, which was putatively attributed to the high selectivity of its CBD. To confirm if the selectivity of EP0 was the same as that of PlyG, fluorescence microscopy was used to analyze different bacteria, including seven *B. thuringiensis* strains, five *B. cereus* strains, one *B. subtilis* strain, one *B. mycoides* strain, one *B. licheniformis* strain, one *B. pumilus* strain, and three other Gram-negative bacterial strains as controls (see Table S2 in the supplemental material). All the above results showed that the truncated fragments of PlyG fused with EGFP still specifically recognized *B. anthracis* cells, consistent with results for the full PlyG protein. Therefore, EP0 and EP3 were used in the following work to study if the truncated fragments of PlyG could recognize *B. anthracis* spores.

Recognition of *B. anthracis* spores. To test the ability of the recombinant truncated fragments to recognize *B. anthracis* spores, equal numbers of *B. anthracis* spores were mixed with EP0, EP3, and EGFP. As shown in Fig. S3 in the supplemental material, only EP0 displayed an obvious ability to recognize *B. anthracis* spores. In contrast, EP3 and EGFP could not bind to these spores.

Further experiments found that only *B. anthracis* spores showed significantly increased fluorescence after staining with EP0, while other closely related spores, including *B. thuringiensis* spores and *B. cereus* spores, did not show any appreciable increase in fluorescence (data not shown). The specificity of EP0 for *B. anthracis* spores was also analyzed statistically by measuring the total fluorescent intensity of each spore (Fig. 2C), demonstrating that only EP0 could significantly enhance the fluorescence, attributable to its direct recognition of and conjugation to the *B. anthracis* spores.

The binding of EP0 to *B. anthracis* spores showed a rate similar to that of binding to *B. anthracis* cells. After 30 min of staining, the fluorescence of each spore reached a maximum (Fig. 2D).

Previous research found that residues 190 to 199 of PlyG were necessary for its binding activity to *B. anthracis* cells (21). The discovery in our work that only EP0 but not EP3 recognized *B. anthracis* spores implied that the 30 amino acids (CSR30, located from 106 to 135) in EP0 or a portion of them may play a key role in recognizing the spores. To confirm whether a spore binding domain (SBD) exists in PlyG, a further four truncated fragments fused with EGFP, EC3, EC5, EC6, and EC8, and three synthesized peptides, FD13, FD23, and FD24, labeled with FITC, were con-

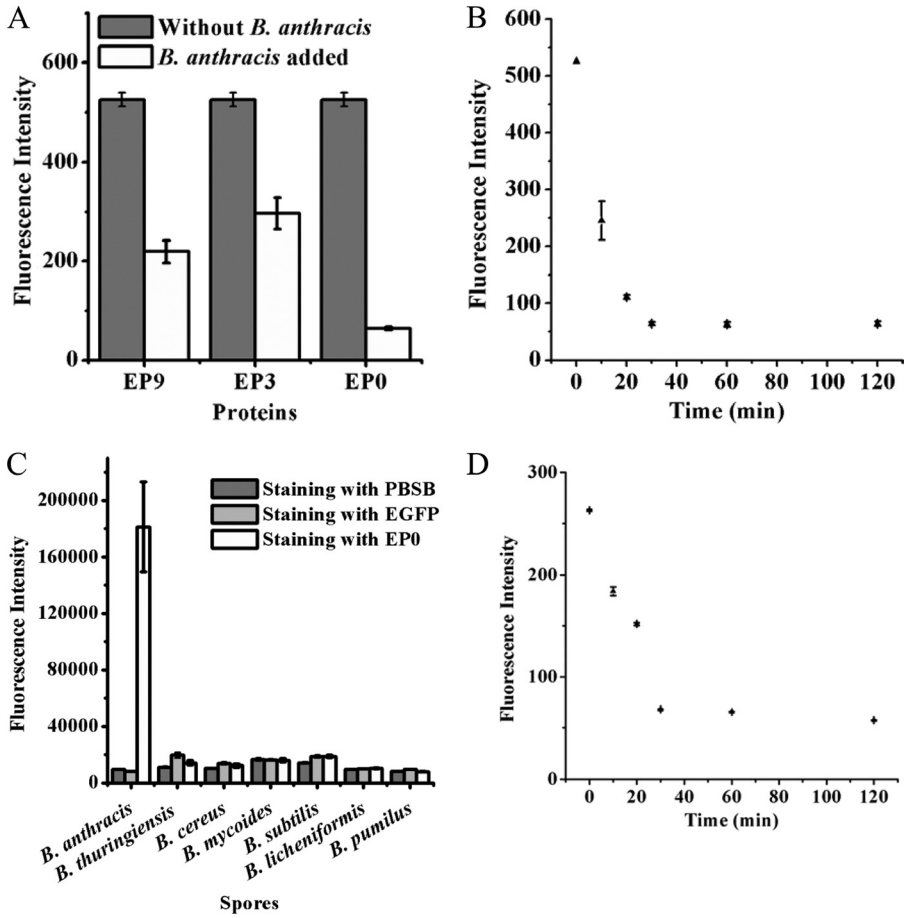

FIG 2 Binding characteristics of the recombinant proteins for *B. anthracis* vegetative cells and spores. (A) Changes in residual fluorescence intensities of EP9, EP3, and EP0 after reaction with *B. anthracis* cells for 30 min. (B) Time gradient of fluorescence changes of the supernatant during reaction of EP0 with *B. anthracis* cells. (C) Specificity of EP0 for *B. anthracis* spores. After staining with EP0, spores were analyzed by the fluorescence microscope system under the same instrument conditions. (D) Time gradient of fluorescence changes of the supernatant during reaction of EP0 with *B. anthracis* spores.

structed to stain the spores and vegetative cells, respectively. As shown in Fig. 3A, the proteins EC5, EC6, and EC8 and the synthetic peptide FD23 could recognize spores but not the vegetative form of *B. anthracis*. The longer peptides, FD13 and FD24, displayed a staining similar to that of FD23 (see Fig. S3 in the supplemental material). To further ensure that the binding between peptide and *B. anthracis* spore is specific but not through charge or hydrophobic interactions, an N-terminally EGFP-fused FD23 peptide (EF3) was constructed and used to stain the spores. The results showed that EF3 could bind tightly to *B. anthracis* spores similarly to the way in which FD23 did (see Fig. S3). What is more, 500 mM Na^+ and 200 mM Mg^{2+}, as well as 200 mM Ca^{2+}, had no influence on binding between EC6 and the spores (data not shown). It is notable that for staining of vegetative cells, FITC can penetrate into heat-treated cells because of its smaller size (Fig. 3A), while FD23 and EGFP cannot.

Additional experiments showed that the full-length PlyG protein fused with EGFP (EG1) recognized the spores and the cells (Fig. 3A), which indicated that the catalytic domain of PlyG did not affect the binding of the truncated PlyG proteins to the spores or vegetative cells.

Further experiments showed that the proteins EP0, EC6, and FD23 also could bind to the sonicated spores, as shown in Fig. 3B. However, the total fluorescence intensity of each sonicated spore stained with EP0 was much lower than that of an intact spore (Fig. 3C). Since sonication can remove part of the exosporium from the spores, the decreased fluorescence may be due to the loss of the exosporium, which indicates that the exosporium of the spores may be the binding target of EP0.

As summarized in Fig. 4, our results showed that recognition of *B. anthracis* vegetative cells and that of its spores were mediated by different domains in PlyG, and a small fragment (residues 125 to 145) was able to bind to the spores.

Analysis of kinetics of binding. Because less is known about the binding characteristics of the spore binding domain (SBD) for *B. anthracis* spores, a fluorescence-based Scatchard plot assay was developed to determine the binding constant and the number of binding sites on a spore. As shown in Fig. 5A, under the same concentration and adding the same number of the spores, of all the truncated proteins, EC6 showed the greatest decrease in fluorescence, which was quite close to that of EG1. This indicated that EC6 had the highest affinity for the spores, and it was identified as the SBD. To create the Scatchard plot, EC6 at a series of concentrations ranging from 0.11 to 1.82 μM was reacted with a constant number of *B. anthracis* spores. The saturation binding data were analyzed using nonlinear regression (Fig. 5C) and displayed in a

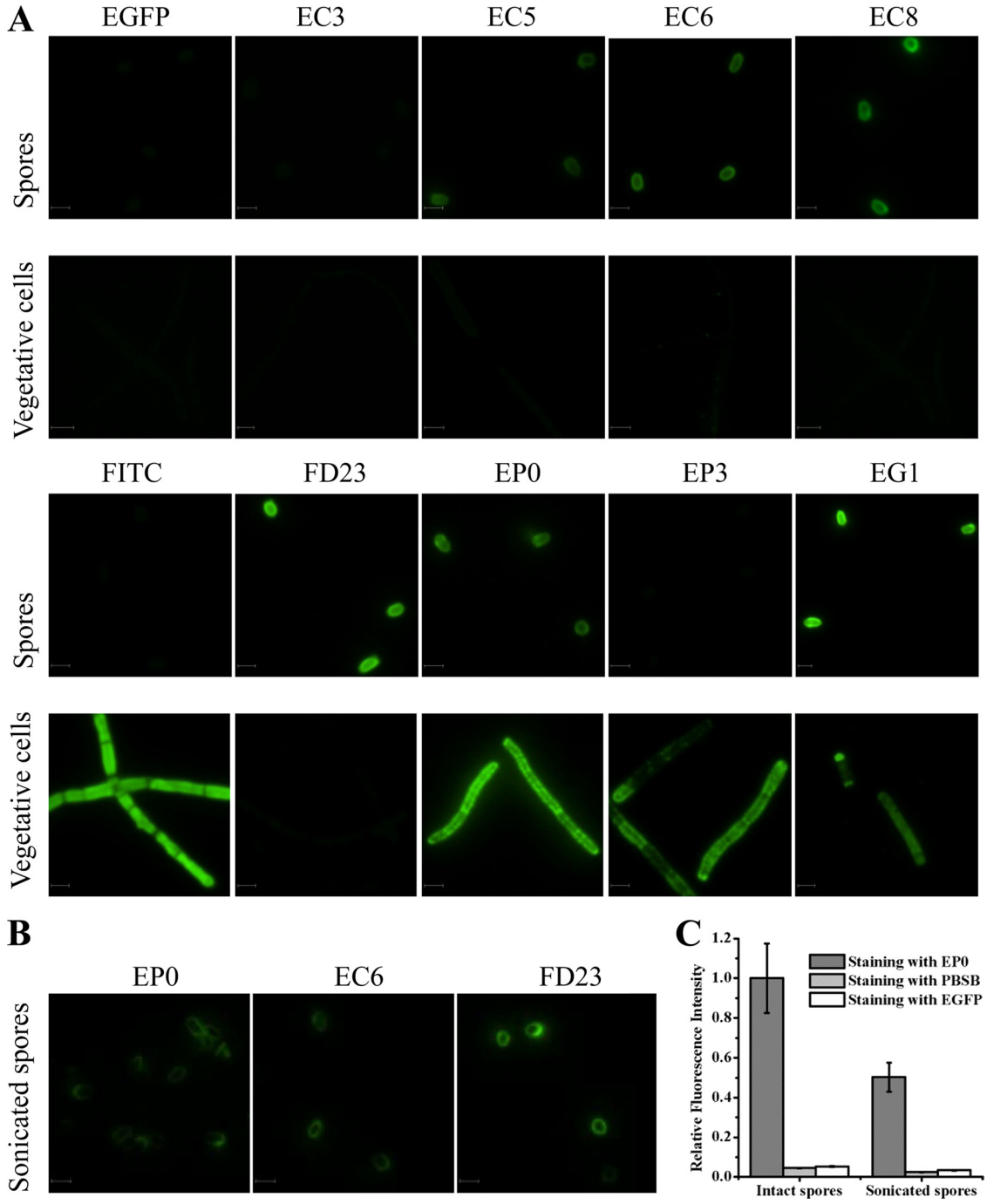

FIG 3 Binding features of the truncated proteins and the peptide for *B. anthracis* spores, heat-treated vegetative cells, and sonicated spores. (A) Binding profiles with *B. anthracis* spores and vegetative cells. (B) Binding profiles with sonicated spores. (C) Relative fluorescence intensities of intact spores and sonicated spores after staining with EP0. All images were taken under the same instrument conditions. Bar = 2 μm.

Scatchard plot, as shown in Fig. 5D, giving a slope of $-2.26\ \mu M^{-1}$ and a y intercept value of $0.47\ \mu M^{-1}$. Therefore, the maximum number of binding sites for EC6 on a spore was found to be 2.1×10^8, and the K_d value of the interaction was 4.4×10^{-7} M.

To analyze the time-resolved dynamic of the interaction between EC6 and *B. anthracis* spores, an Octet apparatus was used to observe the association and dissociation processes. As shown in Fig. 5B, the interaction process presented a slow-association-and-slow-disassociation profile. In addition, the interactions between the truncated proteins EC5, EP0, and EP3 and *B. anthracis* spores were also tested in the Octet system (see Fig. S4 in the supplemental material). Consistent with the SPF data, EC6 displayed a higher affinity for the spores.

PlyG-mediated spore killing. To explore the possible role of SBD on PlyG activity, PlyG with a high lysin activity against *B. anthracis* vegetative cells was obtained after purification by two-

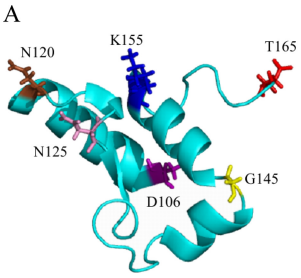

B

Name	Residues	Binding Activity	
		Spores	Cells
EC3	106 to 135	-	-
EC5	106 to 155	+	-
EC6	106 to 165	+	-
FD13	106 to 145	+	-
FD24	120 to 155	+	-
FD23	125 to 145	+	-

FIG 4 Structure-based analysis of the truncated fragments within the SBD. (A) Structure of the PlyG SBD based on the structure of the catalytic domain of PlyG (PDB 2L47_A; GI 350610326). All of the truncated sites are labeled with different colors. (B) Summarized binding results for the truncated fragments within the SBD.

step ion-exchange chromatography (Fig. 6A). In the spore killing assay, the heat-activated spores were mixed with 10 U of PlyG in the presence of 100 mM L-alanine or D-alanine for up to 2 h. When the treatment time was 5 min or 30 min, the decrease in the number of CFU/ml was about 1 log in the presence of either L-alanine or D-alanine. These results indicate that PlyG can bind to the spores, germinating (in the presence of L-alanine) or not (in the presence of D-alanine), hence resulting in almost the same reduced number of CFU (Fig. 6B). Although the reduction in the number of CFU/ml after treatment for 2 h was about 2 logs in the presence of L-alanine, this may be because some of the spores had germinated to vegetative cells and were killed during the exposure. To eliminate the possible influence of L-Ala and D-Ala on the killing efficiency of PlyG through interference with binding of

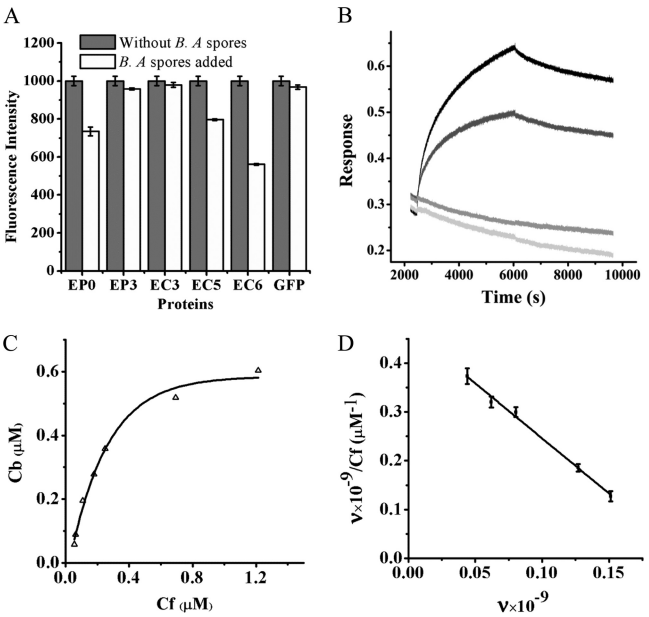

FIG 5 Characteristics of EC6 association with *B. anthracis* (*B. A*) spores. (A) Differences in binding of the truncated proteins to *B. anthracis* spores with the same concentrations and conditions. (B) Kinetics of EC6 association with *B. anthracis* spores at concentrations of 674.6 nM (black) and 337.3 nM (dark gray). EGFP (304.4 nM; gray) and PBS (light gray) were used as the control and the blank, respectively. (C) Saturation binding curve of EC6, shown by the molar concentration of Cf relative to Cb. (D) Simulated Scatchard plot for EC6 association with *B. anthracis* spores (adjusted $r^2 = 0.9918$).

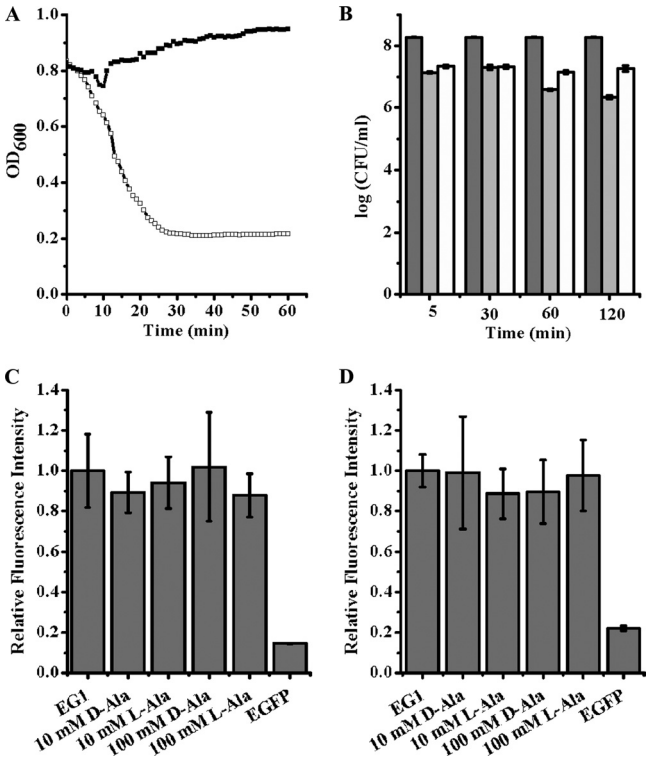

FIG 6 PlyG-mediated spore binding and killing. (A) Lysin activity of PlyG on *B. anthracis* vegetative cells. One unit of two-step-purified PlyG (open squares) displays high activity against *B. anthracis* cells, in contrast to the buffer control (solid squares). (B) Effect of PlyG on *B. anthracis* spores. Heat-activated *B. anthracis* spores were treated with PlyG (10 U) in the presence of either 100 mM L-alanine (light gray) or D-alanine (white) for different times. The resulted CFU were counted and are contrasted with results for the blank control (gray). EG1 can bind to inactivated (C) or live (D) *B. anthracis* spores in the presence of either L-alanine or D-alanine, and the relative fluorescence intensity is not obviously different from that of the buffer control.

PlyG to *B. anthracis* spores, spores, inactivated or not, were stained with EG1 in the presence of different concentrations of L-alanine and D-alanine, respectively. The statistical fluorescence intensity of alanine-treated spores had no obvious difference from that of the untreated control, either inactivated (Fig. 6C) or not (Fig. 6D). These results showed that alanine does not interfere with the binding of PlyG to the spores.

Transmission electron microscopy. To further identify the binding sites of SBD on *B. anthracis* spores, the N21 peptide-labeled AuNPs, N21-AuNPs, were used to stain spores. The maximum absorption of the conjugated N21-AuNPs had a 10-nm red shift relative to that of the bare AuNPs (see Fig. S5 in the supplemental material). Transmission electron microscopy showed that N21-AuNP particles were located mainly on the exosporium of the spores (Fig. 7). Together with the fluorescence results for the sonicated spores in Fig. 3B and C, the exosporium is identified as the most probable binding target of the SBD.

DISCUSSION

Possible impact on mechanism of PlyG activity. As shown in Fig. 3A, our study shows that PlyG uses different domains to recognize the spores and the vegetative cells. The SBD of PlyG contains 60 amino acids, from residue 106 to residue 165. According to the

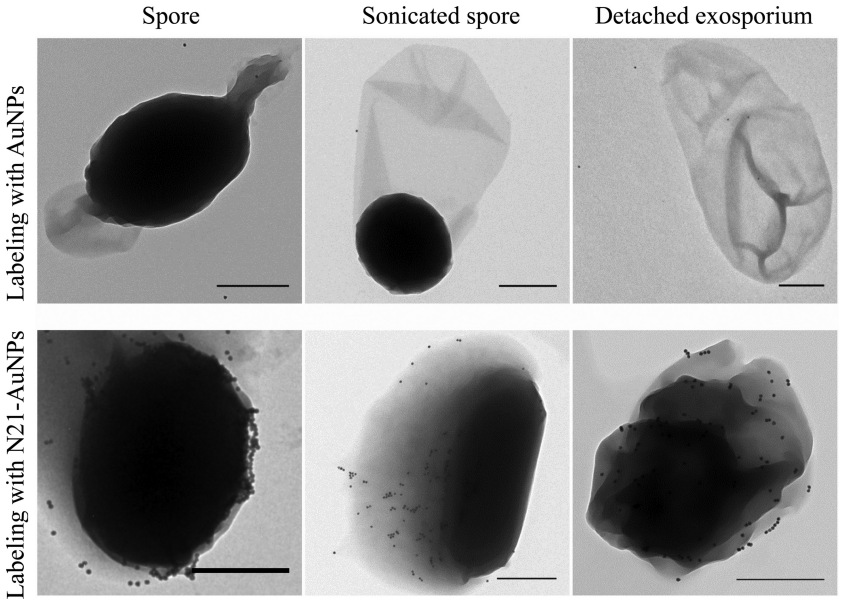

FIG 7 Transmission electron microscopy pictures of *B. anthracis* spores, sonicated spores, and the detached exosporium labeled with bare AuNPs and N21-AuNPs, respectively. Bar = 500 nm.

recently reported structure of the catalytic domain of PlyG (PDB 2L47_A; GI 350610326), the SBD consists of three helixes, 106 to 118 (Hex1), 138 to 145 (Hex2), and 147 to 156 (Hex3), and a sheet from 125 to 129 (Fig. 4A). The fact that EC5, EC6, and FD23 but not EC3 and EP3 retain the ability to recognize *B. anthracis* spores implies that the sheet and Hex2 are the inner core of SBD, while Hex1 and Hex3 are expanded elements that help to bind the spore tighter.

The transmission electron microscopy assays and fluorescence assays of the sonicated spores indicated that the binding sites of the newly identified SBD are most probably on the exosporium of the spores. This result differs from that in a previous report, which suggested that PlyG could recognize only the germinating form, but not spores, of *B. anthracis* (9). This contradiction may be because only a shorter C-terminal fragment of PlyG (residues 156 to 233) was studied as the binding domain in the previous research, and the newly identified spore binding domain is located mainly within the catalytic domain previously considered. This finding may offer an important insight for understanding the way PlyG interacts with spores and its use in control of anthrax.

Since PlyG can bind to spores, this also implies that PlyG could be used immediately to reduce the threat of anthrax in suspected exposures to *B. anthracis* spores without the need to wait until spore germination. Otherwise, if PlyG lacked the ability to bind to spores, early administration of PlyG might not be effective. However, our results also showed that PlyG can bring an obvious but only moderate reduction in the number of CFU of *B. anthracis* spores within 30 min, even in the presence of L-alanine, implying that some modification may be needed for PlyG to further enhance its spore-killing activity.

Biological significance of the spore recognition property of PlyG. The finding that PlyG uses different domains to recognize the spores and vegetative cells might also be a great help in understanding the coevolution of gamma phage with *B. anthracis*. since lysins are used by bacteriophages to digest the bacterial cell wall for the release of progeny virions, it is easy to understand why PlyG can lyse the vegetative cells of *B. anthracis* through the specific recognition of its CBD. However, it is intriguing that PlyG has a special domain for recognizing the spores. It is well understood that spore formation is a special strategy used by bacteria to escape difficult survival conditions. *B. anthracis* bacteria are in a dormant state after forming spores, which is not suitable for replication of gamma phage. Given the fact that the SBD of PlyG is located near the catalytic domain and has a good binding affinity for spores, one possible reason may be that binding of PlyG to spores limits the free diffusion and hence the activity of PlyG for other vegetative cells. This may be helpful in keeping an ecological balance between gamma phage and *B. anthracis* when PlyG is overreleased in the moment of progeny virions' outburst, which could be a new defense mechanism of the exosporium to help the spore survive. Furthermore, it is worth examining whether bacteriophage lysins for other spore-forming bacteria have similar separate domains for recognizing spores and cells.

High specificity of SBD enables rapid identification of *B. anthracis* spores. The newly discovered spore binding domain also provides a good biomarker for identifying the structure of *B. anthracis* spores and for specific detection of the spores. Through studying the targets of the SBD, the cell changes during spore formation in *B. anthracis* could be identified, and hence the structural differences between *B. anthracis* spores and closely related spores, such as *B. thuringiensis* spores and *B. cereus* spores, could be isolated.

Given the potentially lethal threats, rapid identification of *B. anthracis* vegetative cells and its spores is of critical importance. Many methods have been developed in order to do this, including conventional culture assays (45–47), peptide-based assays (1, 19, 24, 53), single-chain antibody-based assays (28, 30, 48, 51), and PCR-based assays (6, 23, 25, 35, 41). However, most of these methods are not able to discriminate between spores and vegetative cells. According to our results, the SBD of PlyG pro-

vides new opportunities for developing better assays for identifying *B. anthracis* spores in view of its high specificity and good affinity. Taking it together with the CBD, one could use either one or two of the domains to recognize spores, the vegetative form of *B. anthracis*, or both in tandem. Furthermore, these highly evolved binding domains target the elements essential for viability, implying a low chance of bacterial mutation to avoid these recognitions.

ACKNOWLEDGMENTS

This work was supported by grants from the basic research program of the Ministry of Science and Technology of China (2012CB721102) to J. Yu and H. Wei, the Infectious Disease Control Research Program of the Ministry of Health of China (2008ZX10004-004 and 2009ZX10003-019), and the National Natural Science Foundation of China (2077508).

We thank Jin He of Huazhong Agricultural University for his kind help in preparation of materials and Simon Rayner at Wuhan Institute of Virology, Chinese Academy of Sciences, for his suggestions and kind help in checking the English of the manuscript.

REFERENCES

1. **Acharya G, et al.** 2007. Label-free optical detection of anthrax-causing spores. J. Am. Chem. Soc. **129**:732–733.
2. **Brumlik MJ, et al.** 2001. Use of long-range repetitive element polymorphism-PCR to differentiate *Bacillus anthracis* strains. Appl. Environ. Microbiol. **67**:3021–3028.
3. **Clery-Barraud C, Gaubert A, Masson P, Vidal D.** 2004. Combined effects of high hydrostatic pressure and temperature for inactivation of *Bacillus anthracis* spores. Appl. Environ. Microbiol. **70**:635–637.
4. **Daniel A, et al.** 2010. Synergism between a novel chimeric lysin and oxacillin protects against infection by methicillin-resistant *Staphylococcus aureus.* Antimicrob. Agents Chemother. **54**:1603–1612.
5. **Dixon TC, Meselson M, Guillemin J, Hanna PC.** 1999. Anthrax. N. Engl. J. Med. **341**:815–826.
6. **Drago L, Lombardi A, Vecchi ED, Gismondo MR.** 2002. Real-time PCR assay for rapid detection of *Bacillus anthracis* spores in clinical samples. J. Clin. Microbiol. **40**:4399.
7. **Dwyer KG, et al.** 2004. Identification of *Bacillus anthracis* specific chromosomal sequences by suppressive subtractive hybridization. BMC Genomics **5**:15.
8. **Fischetti VA, Nelson D, Schuch R.** 2006. Reinventing phage therapy: are the parts greater than the sum? Nat. Biotechnol. **24**:1508–1511.
9. **Fujinami Y, Hirai Y, Sakai I, Yoshino M, Yasuda J.** 2007. Sensitive detection of *Bacillus anthracis* using a binding protein originating from gamma-phage. Microbiol. Immunol. **51**:163–169.
10. **Garcia-Patrone M, Tandecarz JS.** 1995. A glycoprotein multimer from *Bacillus thuringiensis* sporangia: dissociation into subunits and sugar composition. Mol. Cell. Biochem. **145**:29–37.
11. **Gerhardt P, Ribi E.** 1964. Ultrastructure of the exosporium enveloping spores of *Bacillus cereus.* J. Bacteriol. **88**:1774–1789.
12. **Hachisuka Y, Kojima K, Sato T.** 1966. Fine filaments on the outside of the exosporium of *Bacillus anthracis* spores. J. Bacteriol. **91**:2382–2384.
13. **Helgason E, et al.** 2000. *Bacillus anthracis*, *Bacillus cereus*, and *Bacillus thuringiensis*-–one species on the basis of genetic evidence. Appl. Environ. Microbiol. **66**:2627–2630.
14. **Henriques AO, Beall BW, Roland K, Moran CP, Jr.** 1995. Characterization of *cotJ*, a sigma E-controlled operon affecting the polypeptide composition of the coat of *Bacillus subtilis* spores. J. Bacteriol. **177**:3394–3406.
15. **Higgins JA, et al.** 2003. A field investigation of *Bacillus anthracis* contamination of U.S. Department of Agriculture and other Washington, D.C., buildings during the anthrax attack of October 2001. Appl. Environ. Microbiol. **69**:593–599.
16. **Hill HD, Mirkin CA.** 2006. The bio-barcode assay for the detection of protein and nucleic acid targets using DTT-induced ligand exchange. Nat. Protoc. **1**:324–336.
17. **Inglesby TV, et al.** 1999. Anthrax as a biological weapon: medical and public health management. Working Group on Civilian Biodefense. JAMA **281**:1735–1745.
18. **Kailas L, et al.** 2011. Surface architecture of endospores of the *Bacillus cereus/anthracis/thuringiensis* family at the subnanometer scale. Proc. Natl. Acad. Sci. U. S. A. **108**:16014–16019.
19. **Kaman WE, et al.** 2011. Peptide-based fluorescence resonance energy transfer protease substrates for the detection and diagnosis of Bacillus species. Anal. Chem. **83**:2511–2517.
20. **Keim P, et al.** 2001. Molecular investigation of the Aum Shinrikyo anthrax release in Kameido, Japan. J. Clin. Microbiol. **39**:4566–4567.
21. **Kikkawa H, Fujinami Y, Suzuki S, Yasuda J.** 2007. Identification of the amino acid residues critical for specific binding of the bacteriolytic enzyme of gamma-phage, PlyG, to *Bacillus anthracis.* Biochem. Biophys. Res. Commun. **363**:531–535.
22. **Kikkawa HS, Ueda T, Suzuki S, Yasuda J.** 2008. Characterization of the catalytic activity of the gamma-phage lysin, PlyG, specific for *Bacillus anthracis.* FEMS Microbiol. Lett. **286**:236–240.
23. **Kim K, et al.** 2005. Rapid genotypic detection of *Bacillus anthracis* and the *Bacillus cereus* group by multiplex real-time PCR melting curve analysis. FEMS Immunol. Med. Microbiol. **43**:301–310.
24. **Knurr J, et al.** 2003. Peptide ligands that bind selectively to spores of *Bacillus subtilis* and closely related species. Appl. Environ. Microbiol. **69**:6841–6847.
25. **Kumar S, Tuteja U.** 2009. Detection of virulence-associated genes in clinical isolates of *Bacillus anthracis* by multiplex PCR and DNA probes. J. Microbiol. Biotechnol. **19**:1475–1481.
26. **Lai EM, et al.** 2003. Proteomic analysis of the spore coats of *Bacillus subtilis* and *Bacillus anthracis.* J. Bacteriol. **185**:1443–1454.
27. **Loeffler JM, Nelson D, Fischetti VA.** 2001. Rapid killing of *Streptococcus pneumoniae* with a bacteriophage cell wall hydrolase. Science **294**:2170–2172.
28. **Long GW, O'Brien T.** 1999. Antibody-based systems for the detection of *bacillus anthracis* in environmental samples. J. Appl. Microbiol. **87**:214.
29. **Low LY, Yang C, Perego M, Osterman A, Liddington RC.** 2005. Structure and lytic activity of a *Bacillus anthracis* prophage endolysin. J. Biol. Chem. **280**:35433–35439.
30. **Mabry R, et al.** 2006. Detection of anthrax toxin in the serum of animals infected with *Bacillus anthracis* by using engineered immunoassays. Clin. Vaccine Immunol. **13**:671–677.
31. **Moberly BJ, Shafa F, Gerhardt P.** 1966. Structural details of anthrax spores during stages of transformation into vegetative cells. J. Bacteriol. **92**:220–228.
32. **Nelson D, Loomis L, Fischetti VA.** 2001. Prevention and elimination of upper respiratory colonization of mice by group A streptococci by using a bacteriophage lytic enzyme. Proc. Natl. Acad. Sci. U. S. A. **98**:4107–4112.
33. **Nicholson WL, Galeano B.** 2003. UV resistance of *Bacillus anthracis* spores revisited: validation of *Bacillus subtilis* spores as UV surrogates for spores of *B. anthracis* Sterne. Appl. Environ. Microbiol. **69**:1327–1330.
34. **Norby JG, Ottolenghi P, Jensen J.** 1980. Scatchard plot: common misinterpretation of binding experiments. Anal. Biochem. **102**:318–320.
35. **Qi Y, et al.** 2001. Utilization of the *rpoB* gene as a specific chromosomal marker for real-time PCR detection of *Bacillus anthracis.* Appl. Environ. Microbiol. **67**:3720–3727.
36. **Qiao YM, et al.** 2007. Loop-mediated isothermal amplification for rapid detection of *Bacillus anthracis* spores. Biotechnol. Lett. **29**:1939–1946.
37. **Redmond C, Baillie LW, Hibbs S, Moir AJ, Moir A.** 2004. Identification of proteins in the exosporium of *Bacillus anthracis.* Microbiology **150**:355–363.
38. **Roth IL, Williams RP.** 1963. Comparison of the fine structure of virulent and avirulent spores of *Bacillus Anthracis.* Tex. Rep. Biol. Med. **21**:394–399.
39. **Sainathrao S, Mohan KV, Atreya C.** 2009. Gamma-phage lysin PlyG sequence-based synthetic peptides coupled with Qdot-nanocrystals are useful for developing detection methods for *Bacillus anthracis* by using its surrogates, *B. anthracis*-Sterne and *B. cereus*-4342. BMC Biotechnol. **9**:67.
40. **Schuch R, Nelson D, Fischetti VA.** 2002. A bacteriolytic agent that detects and kills *Bacillus anthracis.* Nature **418**:884–889.
41. **Sohni Y, Kanjilal S, Kapur V.** 2008. Performance evaluation of five commercial real-time PCR reagent systems using TaqMan assays for *B. anthracis* detection. Clin. Biochem. **41**:640–644.
42. **Sonenshein AL, Cami B, Brevet J, Cote R.** 1974. Isolation and characterization of rifampin-resistant and streptolydigin-resistant mutants of *Bacillus subtilis* with altered sporulation properties. J. Bacteriol. **120**:253–265.
43. **Sylvestre P, Couture-Tosi E, Mock M.** 2002. A collagen-like surface glycoprotein is a structural component of the *Bacillus anthracis* exosporium. Mol. Microbiol. **45**:169–178.

44. **Takahashi H, et al.** 2004. *Bacillus anthracis* incident, Kameido, Tokyo, 1993. Emerg. Infect. Dis. **10**:117–120.
45. **Titball RW, Turnbull PC, Hutson RA.** 1991. The monitoring and detection of *Bacillus anthracis* in the environment. Soc. Appl. Bacteriol. Symp. Ser. **20**:9S–18S.
46. **Turnbull PC.** 1991. Anthrax vaccines: past, present and future. Vaccine **9**:533–539.
47. **Turnbull PC.** 1999. Definitive identification of *Bacillus anthracis*—a review. J. Appl. Microbiol. **87**:237–240.
48. **Wang DB, et al.** 2009. Label-free detection of *B. anthracis* spores using a surface plasmon resonance biosensor. Analyst **134**:738–742.
49. **Wang DB, et al.** 2009. Detection of *B. anthracis* spores and vegetative cells with the same monoclonal antibodies. PLoS One **4**:e7810. doi:10.1371/journal.pone.0007810.
50. **Wang J, et al.** 2005. 2-D reference map of *Bacillus anthracis* vaccine strain A16R proteins. Proteomics **5**:4488–4495.
51. **Wang SH, et al.** 2006. Construction of single chain variable fragment (ScFv) and BiscFv-alkaline phosphatase fusion protein for detection of *Bacillus anthracis.* Anal. Chem. **78**:997–1004.
52. **Weder HG, Schildknecht J, Lutz RA, Kesselring P.** 1974. Determination of binding parameters from Scatchard plots. Theoretical and practical considerations. Eur. J. Biochem. **42**:475–481.
53. **Williams DD, Benedek O, Turnbough CL, Jr.** 2003. Species-specific peptide ligands for the detection of *Bacillus anthracis* spores. Appl. Environ. Microbiol. **69**:6288–6293.
54. **Yang H, He J, Hu F, Zheng C, Yu Z.** 2010. Detection of *Escherichia coli* enoyl-ACP reductase using biarsenical-tetracysteine motif. Bioconjug. Chem. **21**:1341–1348.